ARCHIVES OF
IRANIAN
MEDICINE

Open Access

Original Article

Accuracy of Magnetic Resonance Spectroscopy Techniques in Prostate Cancer and Prostatitis

Mansour Zabihzadeh, PhD[1,2,3]; Jafar Fatahi Asl, PhD[4]; Zahra Farzanegan, MSc[2*]; Seyed Mokhtar Hoseini, MD[5]; Mohsen Sarkarian, MD[5]; Bahman Cheraghian, PhD[6]; Shapour Dahaz, PhD[7]; Mohammad Momen Garibvand, MD[8]

[1]Cancer Research Center, Ahvaz Jundishapur University of Medical Sciences, Ahvaz, Iran
[2]Department of Medical Physics, School of Medicine, Ahvaz Jundishapur University of Medical Sciences, Ahvaz, Iran
[3]Department of Clinical Oncology, Golestan Hospital, Ahvaz Jundishapur University of Medical Sciences, Ahvaz, Iran
[4]Department of Radiology, School of Para Medicine, Ahvaz Jundishapur University of Medical Sciences, Ahvaz, Iran
[5]Department of Urology, School of Medicine, Ahvaz Jundishapur University of Medical Sciences, Ahvaz, Iran
[6]Department of Biostatistics and Epidemiology, School of Public Health, Ahvaz Jundishapur University of Medical Sciences, Ahvaz, Iran
[7]Department of Anatomy, School of Medicine, Ahvaz Jundishapur University of Medical Sciences, Ahvaz, Iran
[8]Department of Radiology, School of Medicine, Ahvaz Jundishapur University of Medical Sciences, Ahvaz, Iran

Abstract

Background: Considering the non-invasive nature of magnetic resonance spectroscopy (MRS) and its ability to detect prostate lesions, the present study aimed to investigate the accuracy of MRS techniques in distinguishing between prostate cancer (PCa) and prostatitis.

Methods: Thirty-three patients (18 patients with PCa and 15 patients with prostatitis) were recruited for this study. Magnetic resonance imaging (MRI) and MRS were performed using 1.5-T system GE- modle Optima 450 Discovery (GE Medical Systems, US). The (Cho+Cr)/Cit ratio of hypointense T2 areas were calculated. The diagnostic accuracy including sensitivity and specificity indices, with 0.95 confidence interval as well as PPV and NPV were calculated for each variable. The receiver operating characteristic (ROC) area under the curve (AUC) was outlined and investigated. The mean quantitative values between the two groups (PCa and Prostatitis) were compared using independent t test.

Results: The mean ratios of Cho+Cr/Cit in PCa was 1.54 ± 0.63 and 0.83 ± 0.48 for PCa and prostatitis, respectively, indicating a significant statistical difference ($P = 0.00$). A reduction in citrate was seen in both PCa and prostatitis tissue. Significant elevation in choline peak was shown for PCa. Moreover, creatinine level was low in both normal tissue and PCa without significant difference. Sensitivity, specificity, accuracy, PPV and NPV of MRS were 94.4% (95% CI, 74.2–99), 80% (95% CI, 54.8–93), 96%, 85% and 92.4%, respectively.

Conclusion: The results of this study indicate an acceptable level of sensitivity, specificity and accuracy of MRS in the differential diagnosis of PCa and prostatitis.

Keywords: Magnetic resonance spectroscopy, Prostate cancer, Prostatitis

Cite this article as: Zabihzadeh M, Fatahi Asl J, Farzanegan Z, Hoseini SM, Sarkarian M, Cheraghian B, et al. Accuracy of magnetic resonance spectroscopy techniques in prostate cancer and prostatitis. Arch Iran Med. 2020;23(2):104–112.

Introduction

Prostate cancer (PCa) is one of the most common cancers and the sixth leading cause of cancer deaths in the world. This disorder is very non-uniformly distributed and is more prevalent in developed countries such as Australia, North America and Europe.

Although the risk factors associated with PCa are not well known, age, ethnicity and inheritance can be considered, since if one of the first-degree relatives is afflicted, the likelihood of the disease doubles.[1] Prostate lesions are mainly associated with clinical symptoms such as enuresis, increased urinary frequency and increased prostatic specific antigen.[2] PCa and benign prostatic hyperplasia have a focal presentation, while prostatitis is a diffuse disease. However, the clinical symptoms of all three diseases are similar.[3]

Common clinical tests for the examination and detection of PCa include investigating the concentration of prostate specific antigens (PSAs) in blood serum, rectal examination, and transrectal ultrasonography (TRUS)-guided biopsy.[4] Although PSA blood test is the most common method for early diagnosis of PCa, this method has a low level of specificity. Furthermore, there is also a risk of PCa, even in people with normal antigen levels (<4 ng/mL), and an increased PSA levels is also observed in benign prostate lesions.[5] The rectum examination only allows palpation of the posterior prostate part, and its sensitivity and specificity are not suitable for monitoring treatment. In case of obtaining suspicious results from prostatic specific antigen and rectal examination, TRUS-guided biopsy is used as an invasive and complementary method for histological investigation.[6]

***Corresponding Author:** Zahra Farzanegan MSc, Department of Medical Physics, School of Medicine, Ahvaz Jundishapur University of Medical Sciences, Golestan Blvd., Ahvaz 61357-33118, Iran. Tel: +98- 918-5929185; E-mail: farzanegan.z97@gmail.com

Biopsy is accompanied by bleeding and an increased risk of infection. Therefore, it should be replaced by a non-invasive method with high sensitivity and specificity.[6,7]

Magnetic resonance imaging (MRI) is a non-invasive imaging technique in which no ionizing radiation is used. This modality is capable of depicting PCa, and provides anatomical and physiological information for diagnosis, staging, and treatment planning.[7,8] Different types of MRI for diagnosing prostate lesions include: T2-weighted imaging, diffusion-weighted imaging (DWI), dynamic contrast enhanced MRI (DCE-MRI) and magnetic resonance spectroscopy (MRS), conventional DWI and T2-weighted imaging methods have the ability to detect large tumors; however, they are limited in the detection of small-size tumors. Moreover, dynamic contrast enhanced MRI is also an effective method for detecting abnormalities.[9,10] Among the different MRI techniques, MRS as a functional non-invasive study allows the examination of the levels of prostate metabolites including citrates, polyamines, choline contents, creatinine and phosphocreatine. Accordingly, MRS has the ability to detect PCa and differentiate it from other benign lesions.[11] The concentration of metabolites is usually expressed in parts per million (ppm) and measured using chemical shift imaging protocol with suppression of water signals and unwanted fat signals in the desired volume. Metabolites related to PCa include citrate (benign tissue marker), creatinine (not individually important for diagnosis, and its peak is usually hard to distinct from choline) and choline (marker for malignant tissue). The estimation of peak integrals of all metabolites in a quantitative analysis is carried out by the ratio of the sum of choline and creatinine to citrate (Cho+Cr/Cit).[3,12-14] If this ratio is higher than 0.72 in at least two adjacent vascular tissues, a malignant tumor marker is considered, while the ratio between 0.58 and 0.72 is considered to be ambiguous. In qualitative analysis, the height of peak for citrate and choline is compared visually, which would be suspicious for PCa if the higher peak choline/creatinine ratio was observed in at least three adjacent voxels.[15] Regarding the non-invasive nature, sensitivity and specificity of MRS and its ability to detect small tumors in the early stages, this study was conducted to determine the ability of MRS to distinguish between PCa and prostatitis.

Materials and Methods
Patients and Data
Between May of 2018 and January of 2019, 33 male patients were referred to Ahvaz Arya MRI center, aged 51 to 88 years old with a mean age of 65.53 years. In order to determine the sample size, the diagnostic test evaluation formula [n (se) $=z_{1-\alpha/2}^2 \times$ se (1-se)/$d^2 \times$ prev and n (sp) $=z_{1-\alpha/2}^2 \times$ sp (1-sp)/$d^2 \times$ (1-prev)] was used, where, $\alpha = 0.05$, and based on the results of previous similar studies,[16] sensitivity = 96.1%, specificity = 96.5% and accordingly, d = 0.15 and based on pilot study results (percentage of patients with PSA higher than 4 who had cancer after biopsy), $P = 0.2$ were considered. Based on these parameters, the sample size was calculated at 33 patients. The non-probability simple sampling method using Stata 13.0 software, as well as reference articles[17-19] were used to select the sample size. The diagnosis of PCa was suspected by the measurement of serum prostate-specific antigen level and confirmed using TRUS-guided biopsy.

Eighteen patients had PCa (average age of 67.77 years with range of 51–88 years), and 15 patients had prostatitis (average age 62.16 years with range of 55–69 years). The mean level of PSA of all patients was 11.01 ng/mL (15.25 for PCa and 4.66 for prostatitis patients). All patients successfully underwent routine MRI and 3D MRS after prostate biopsy. TRUS-guided biopsy proved prostatitis and PCa. The exclusion criteria were: 1) metallic implants or pacemaker, 2) claustrophobic patients, 3) urinary tract infection, 4) unwillingness to participate in the study, 5) prior PCa treatment (hormonal, surgical and/or radiation therapy), or prior antibiotic treatment. The mean time between biopsy and MRI was 3 to 6 months.

MRI Protocol
All MRI tests were performed using 1.5 T scanner GE-model Optima 450 Discovery (GE Medical Systems, USA). In order to stimulate the desired area by RF pulse, a radiofrequency body coil was used and the data acquisition was performed using a pelvic phased array coil. With the aim of determining the range and location of the tumor and the scope for the spectroscopy, T 2 fast-spin echo technique (T2WI) was implemented, which included: TR = 3000 ms, TE = 100 ms, FOV of 18 × 18 cm², 3 mm section thickness, 0.6 mm intersection gap, matrix size of 300 × 300, number of excitation (NEX) of 8. Acquisition was begun with obtain three planes.

Spectroscopic Data Acquisition
With the aim of evaluating the total volume of the prostate and determining the appropriate range for spectroscopy, the MRS programming included T2-weighted (fast spin echo) sequences. After anatomical images of axial, coronal and sagittal projections were acquired in which positioning the volume of interest on the images showed the largest diameter of the prostate in all three planes. Spectroscopic data acquisition was performed using 3D-chemical shift imaging (TR = 3000 ms, TE = 35 ms, FOV = 24 × 24 cm² and voxel size of 0.10–0.22 cm³). In the MRS technique, eight external saturation bands were used to prevent field non-homogeneity and magnetic susceptibility that was associated with the presence of air in the coil, bone structures, prostate-surrounding fat, and presence of urine in the bladder (Figure 1). Spectral suppression of water and fat in the prostate MRS
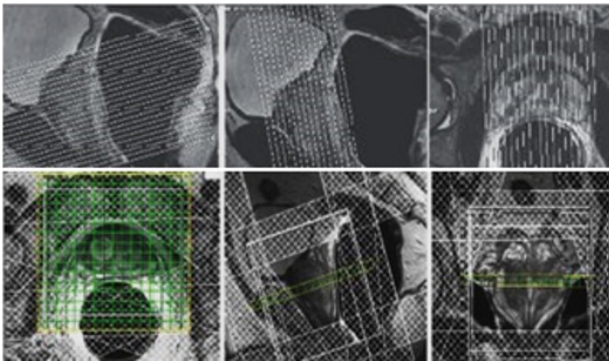
Figure 1. Section Selection and Saturation Bands Position.

leads to non-interference of these structures in the scan. Saturation-bands were positioned in all directions around the prostate in order to eliminate disturbances of the spectra caused by periprostatic tissue, fat tissue, and rectum tissue. The local magnetic field homogeneity was optimized with auto-shimming procedure (Figure 2). In general, the time required to complete the scan including patient positioning, MR imaging and spectroscopic data acquisition was about 35 minutes. The average spectroscopy scanning time was about 17 minutes.

Data Interpretation
T2W Analysis
Data were transferred to workstation for final curve of each voxel. To correct all images related to the profiles received from the pelvic phased array coil, a PACS workstation (UniSight, EBM-PACS; Taiwan) was used. Images were reviewed by an experienced radiologist who did not know the histopathologic findings of the patients. T2 images were used to assess the entire prostate gland and the surrounding tissue. Accordingly, the suspicious hypo-intense areas that were indicative of cancerous or inflammatory tissue were localized.

MR Spectroscopic Analysis
In hypo-intense T2 area, the ratio of Cho+Cr/Cit was calculated in both prostate inflammatory and cancerous tissues using prostate spectroscopy and imaging examination sequence. In addition to metabolite ratios, the citrate and choline amplitudes in hypo-intense T2 area were compared with that of normal tissue. The studies were consensually
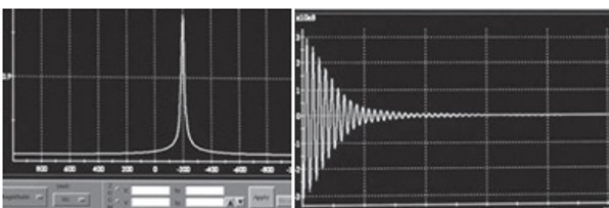

Figure 2. Auto-shimming Procedure.

evaluated by an expert radiologist regarding the morphology and spectral analysis. Qualitative analysis of total prostate volume was performed. Initially, areas that included increased levels of choline and decreased citrate levels were considered as target areas. Eventually, a qualitative and quantitative assessment was conducted to determine the relationship between metabolite peak amplitude ratios in the target area. Lesions with Cho+Cr/Cit ratios more than 0.58 were classified as malignant lesions according to the recent guideline.[20]

Statistical Analysis
TRUS-guided biopsy was used as the reference standard for this study. Accordingly, the risk of presence or absence of PCa was definitely determined.

SPSS statistical software version 24.0 was used for data analysis. Parameters related to diagnostic accuracy including sensitivity and specificity indices, positive predictive value (PPV) and negative predictive value (NPV) were calculated for each variable with a confidence interval of 95%.

ROC was charted by selecting the PSA and the ratio of Cho+Cr/Cit that were considered as test variables and the existence or absence of cancer (based on biopsy diagnosis) that was rated by 1 and 0 scores considered as a state variable. Based on the ROC curve, the best values for sensitivity and specificity were selected. Accordingly, the values of PPV and NPV were calculated using Stata 13.0 and WINPEPI 3.2.

In addition, the area under the receiver operating characteristic (ROC) curve (AUC) was outlined and investigated from the ROC curve. This value was considered as test accuracy. The mean and standard deviation of the ratio of total choline and creatinine to citrate were calculated for both types of lesion. To investigate the presence or absence of significant difference in the ratio of Cho+Cr/Cit between the two types of lesions, two independent samples t test (two tailed P values) was used. P values of less than 0.05 were considered as significant.

Results
The 33 studied patients were aged 51 to 88 years with a mean age of 65.53 years. Fifteen had benign pathology in transitional zone and 18 had malignant pathology in peripheral locations on the histopathological examination. Thirty-three patients with PC (18 persons) and prostatitis (15 persons) underwent MRI/MRSI. The demographic, clinical and pathological characteristics of the patients are shown in Table 1 (To calculate all values, a confidence interval of 95% was considered and p-value less than 0.05 was significant).

The average of PSA in all patients was 11.01 ± 6.62, which was 15.25 ± 4.90 in PCa and 4.66 ± 2.26 in prostatitis patients. The results of the pathological examination that shows the stage of the cancer with Gleason grading showed

Table 1. Patients' Demographic and Clinicopathological Characteristics

	Prostate Cancer	**Prostatitis**
Patients (n)	18	15
Age (mean)	67.77 ± 10.31	62.16 ± 5.35
PSA (Mean ± SD, ng/mL)	15.25 ± 4.90	4.66 ± 2.26
Gleason score biopsy (n)		
<7	5	
3 + 4	4	
4 + 3	0	
>7	9	

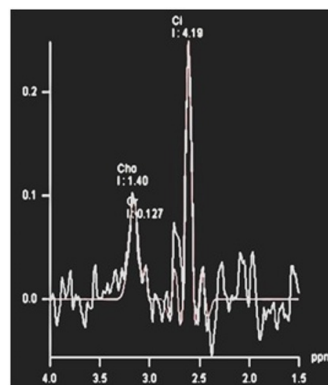CI=95%, *P* value less than 0.05 was significant.

Figure 3. Metabolites in the Normal Prostate Tissue, Indicating a Higher Peak of Citrate Compared with Choline.
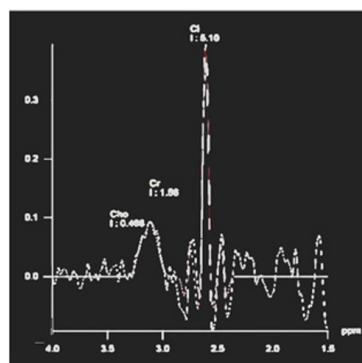

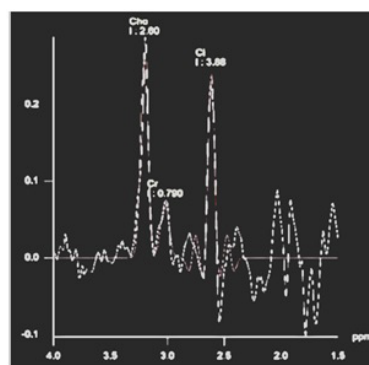**Figure 4**. Metabolite Spectrum of Prostatitis, Increased Choline and Significant Reduction in Citrate.

Figure 5. Metabolite Spectrum of Prostate Cancer Tissue, a Significant Increase in Choline Peak and Decreased Citrate Peak.

that 27.8% (5 persons) had Gleason score <7, 22.20% (4 persons) had Gleason score of 7 and 50% (9 persons) had Gleason score >7. Most patients had Gleason scores above 7 and more advanced stages of the tumor. All carcinomas and prostatitis lesions showed focal or diffuse hypo-intensity on T2WI. The mean Cho+Cr/Cit ratio in cancerous region was 1.54 ± 0.63, and 0.83 ± 0.48 in prostatitis tissue. Accordingly, this ratio was higher in cancer patients than prostatitis patients. The difference between these two gropes was statistically significant ($P < 0.001$) (Table 2). To calculate all values, a confidence interval of 95% was considered and p-value less than 0.05 was significant. For PSA, sensitivity was 100% (95% CI, 82.4–100) and specificity was 73.3% (95% CI, 48.1–89.7). For MRS, sensitivity was 94.4% (95% CI, 74.2–99) and specificity was 80% (95% CI, 54.8–93).

MRS represents the high level of citrate peak in normal prostate tissue (Figure 3); however, decreased levels of this metabolite was observed in both prostatitis and PCa. Choline peak was elevated in case of prostatitis and PCa, which was significant for PCa but not significant for prostatitis compared to the normal tissue. Creatinine level was low in case of normal as well as PCa and there was no significant difference in this regard. The peak values of choline metabolite in the cancerous region were significantly higher than the normal region and the area involved in prostatitis. While the Citrate value was lower in the cancerous regions (Figures 4 and 5).

The sensitivity, specificity, accuracy, PPV and NPVs are shown in Table 2 and Figure 6. Cho+Cr/Cit ratios of the malignant lesions in this study ranged from 0.60 to 2.60 with a mean of 1.54. Cho+Cr/Cit ratios of the benign lesions ranged from 0.20 to 0.95 with a mean of 0.48 (Table 2). A significant relationship was observed between Cho+Cr/Cit ratio and clinicopathological characteristics including Gleason score and PSA level ($P < 0.001$ and $P = 0.001$, respectively) (Table 3). There was not any significant

relationship between Cho+Cr/Cit ratio and age in the two types of disease ($P = 0.55$ and $P = 0.83$ for PCa and prostatitis, respectively). In addition, there was not any significant relationship between age and type of disease ($P = 0.57$).

Table 2. Sensitivity and Specificity

Test type	Sensitivity	Specificity	PPV	NPV	Accuracy (AUC)
PSA	100%, 95% CI (82.4–100)	73.3%, 95% CI (48.1–89.7)	81.8%	100%	80%
MRS	94.4%, 95% CI (74.2–99)	80%, 95% CI (54.8–93)	85%	92.4%	96%

CI=95%, *P* value less than 0.05 was significant.

Table 3. Relationship between MRS Results and Clinicopatological Tests

	Gleason score			PSA		
	<7	7	>7	4≥	4–10	>10
Cho+Cr/Cit	0.79 ± 0.11	1.35 ± 0.39	2.04 ± 0.43	0.51 ± 0.07	0.62 ± 0.53	1.58 ± 0.73
P value		<0.001			0.001	

CI=95%, *P* value less than 0.05 was significant.
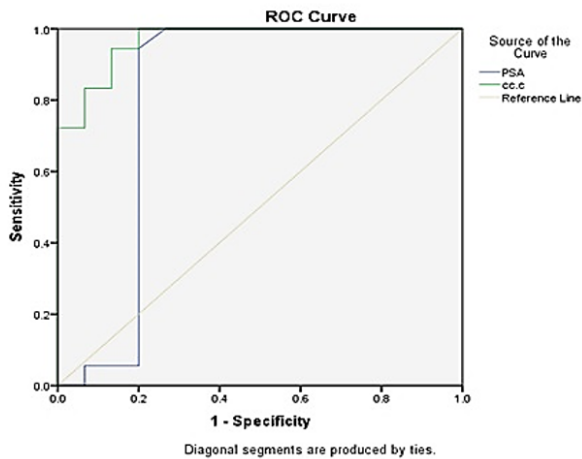
Figure 6. ROC Curve for MRS vs PSA.

Discussion

With the aim of providing information on biochemical and structural changes in the prostate, advanced MRI techniques including MRS have been applied by a number of previous studies.[21-23] Recently, the possibility of creating high-resolution images of the proton spectrum of the total prostate volume was provided using MRI techniques. Based on the results of this and previous studies,[24,25] an increase in choline concentration has been observed in cancerous areas. An increase in the signal of choline containing compounds has been observed in brain tissue tumors, which can be due to the high proliferation rate of tumor cells.[26] According to previous studies,[27-30] the amount of choline in the group of patients with prostatitis is lower than the PCa group and is close to normal level. Significant increases in choline in PCa and no significant alteration in prostatitis have also been reported in other studies.[23,30] Decreased citrate levels in cancerous tissues can be due to decreased citrate secretion epithelial structures.[25,31] Citrate synthesis and secretion are exocrine functions in the prostate which are stimulated by androgenic hormone. Reducing citrate in PCa is due to the reduced ability to produce and secrete it. Generally, malignant epithelial cells are composed of areas occupied by the glandular ducts.[32]

In this study, like other studies,[30] there was a significant difference in the amount of citrate in prostatitis compared to the cancer. Moreover, the creatinine levels were higher in patients with prostatitis than cancer but this difference was not statistically significant, which is consistent with other studies that have not indicated any significant alteration in creatinine levels in patients with PCa.[33]

Comparison of the spectrum for these two groups showed a significant increase in Cho + Cr / Cit ratio in patients with PCa compared with prostatitis (P < 0.05). This result is consistent with a study by Kurhanewicz et al, suggesting an increase in the ratio of total choline and creatinine to citrate in PCa and its reduction in benign lesions.[34] Zhang et al reported a higher proportion of Cho+Cr/Cit ratios in patients with prostatitis; they stated a reduction of the citrate levels in the inflammatory process due to the reduction of luminal space despite no significant changes in choline.[24] Regarding the sensitivity of the test, the values obtained for Cho+Cr/Cit were obtained at 100%. The specificity of the test was 80%. Therefore, sensitivity was higher. Studies by Cirillo et al[35] and Wang et al[36] also highlighted the magnetic resonance spectral sensitivity compared to specificity (95% vs 91%, 84.2% vs. 28.6%, 80.05 % vs 78.46%) which is in agreement with the results of the present study. Chen et al[16] and Amsellem-Ouazana et al[37] reported higher sensitivity values (84.3% vs. 98%. 73.3% vs. 96.3%).

The accuracy of MRS was calculated at about 96%, which is consistent with the results of the study by Chen et al,[16] which reported the accuracy of MRS at about 96%. The MRS accuracy was reported about 75.9%, 88% and 78% by Cirillo et al,[35] Amsellem-Ouazana et al,[37] and Wang et al,[36] respectively. Based on the results of this study, the PPV and NPV of MRS were 85% and 92.4%, respectively which are in accordance with those reported by Amsellem-Ouazana et al[37] and Cirillo et al[35] that suggested NPVs of 88% and 92.9% and PPVs of 86.6% and 87.7%, respectively.

Moreover, this study suggested a significant correlation between the ratio of total choline and creatinine to citrate and the stage of cancer based on Gleason scoring, so that patients with high Gleason score as well as a higher PSA level had a higher Cho+Cr/Cit ratio. This rate was 0.79 ± 0.11, 1.35 ± 0.39 and 0.43 ± 2.04 in patients with Gleason scores of <7, 7 and >7, respectively. In addition, the Cho+Cr/Ci ratio in patients with PSA levels of <4, 4–10 and >10 was 0.07 ± 0.51, 0.53 ± 0.62 and 0.73 ± 1.58, respectively. A significant relationship has been observed between Gleason score, PSA level and the ratio of total choline and creatinine to citrate in other studies. Ghafoori and Rasteh[38] reported higher total amount of choline and creatinine to citrate in higher cancer stages. The same finding can be found for PSAs; higher PSA levels for higher total amounts of choline and creatinine to citrate. Kobus et al[39] showed that by increasing the proportion of Cho+Cr/ Cit, the invasive level of PCa also increases. Cheng et al[40] stated that the profile of MRS metabolites can be helpful in evaluating the pathological stage and the amount of invasive PCa for determining the suitable treatment protocol. Yu et

al[41] declared that spectroscopic examination and evaluation of the ratio of total choline and creatinine to citrate is an acceptable indicator for detection of PCa. The results from other studies regarding the comparison of MRS accuracy with other techniques are shown in Table 4.

In the MRS method, the choice of optimal volume and the exact location for network placement and data acquisition are particularly important. This precision should be such that the matrix is far from the fat and water tissues so that the signal generated by them does not disturb the

data and can be performed with high accuracy. In fact, the homogeneity or uniformity of tissue within the vessels plays a very important role in this kind of diagnostic method. In addition, the smallness of the voxels will reduce possible errors in order to make the texture even more uniform. In this project, the matrix involved the entire region of the tumor or inflammatory lesion, and as far as the spatial resolution of the device allowed, the surrounding areas was not included in the matrix. Verifying these results and their associated assumptions requires a larger sample size study.

Table 4. Comparison of Different Methods with MRS

First Author/Year	Imaging Techniques	Sensitivity	Specificity	PPV	NPV	Accuracy
Mueller-Lisse (2001)[43]	T2WI	75%	60%	—	—	—
	MRS	80%	73%			
Yuen (2004)[44]	T2WI	57.1%	57.1%	100%	88.2%	82.4%
	MRS	70.6%	66.7%	57.1%	58.3%	83.3%
Chen (2008)[16]	T2WI	88.2%	67.2%			
	DWI	82.4%	81.6%	—	—	—
	MRS	96.1%	96.5%			
Sciarra (2008)[45]	DCE	71%	94%	96%	63%	
	MRS	84%	88%	93%	74%	—
Haffner (2011)[46]	TRUS	95%	83%	—	—	88%
	MRS	95%	100%	—	—	98%
Aydin (2012)[47]	T2WI	46%	68%			
	DCE	43%	67%	—	—	—
	DWI	29%	82%			
	MRS	69%	70%			
Caivano (2012)[48]	T2WI	88%	61%	73%	81%	76%
	DWI	88%	61%	73%	81%	76%
	MRS	92%	89%	87%	88%	87%
Roy (2013)[49]	T2WI	57%				
	DCE	54%	—	—	—	—
	DWI	100%				
	MRS	71%				
Cha (2015)[50]	T2WI	82%	75%	35%	96%	
	DCE	48%	89%	41%	91%	
	DWI	83%	86%	50%	96%	—
	MRS	85%	85%	49%	97%	
Kitajima (2015)[51]	T2WI	57%	78%			
	DCE	44%	85%	—	—	—
	DWI	78%	85%			
	MRS	77%	87%			
Vigneault (2016)[52]	DWI	93.7%	82.1%	89.4%	88.9%	
	MRS	98.6%	60.8%	77.3%	96.9%	—
Ahmed (2017)[6]	TRUS	48%	96%	—	—	—
	MRS	93%	41%			
Jaganathan (2017)[17]	DWI	89.5%	85.7%	94.4%	75%	
	MRS	84.2%	28.6%	76.2%	40%	—
Sandgren (2017)[53]	TRUS	94%	100%			
	T2WI	48%	52%			
	DCE	82%	92%	—	—	—
	DWI	82%	89%			
	MRS	84%	88%			

PPV, positive predictive value; NPV, negative predictive value; T2WI, T2 weighted imaging; DCE, dynamic contrast-enhanced; DWI, diffusion-weighted imaging; MRS, magnetic resonance spectroscopy.

In spite of its many benefits, MRI imaging has limitations such as inability to be performed for patients with claustrophobia, or for those with heart pacemakers, aneurysm nodes and other metal objects. In addition, it is very sensitive to the voluntary and unwanted movements of the patient.

Despite the precise physical principles and the clinical capability of MRS, like other MRI techniques, this method has particular limitations. For example, voluntary and involuntary patient movements lead to overall frequency changes, decreased levels of peak metabolites, and reduced quality of water peak suppression, which can be resolved with proper shimming and improved magnetic field strength. Another issue is the truncation artifact that can be eliminated using the appropriate RF receiver system. In addition, the ability to detect microbubbles and metabolites with a short signal decay time is limited by conventional scanners and requires high magnetic field strength and strong gradients.[42]

The small volume of samples is undoubtedly the most important limitation of the study. Verifying these results and their associated assumptions requires a larger sample size study.

This study was performed using phased Array Coil and 1.5T magnetic field intensity. In order to detect more metabolites in higher magnetic fields and increase the resolution of MRS, it is suggested that this study is repeated with a system with higher magnetic field intensity and using endorectal coil. Studying the other metabolites as new biomarkers that may appear during a higher intensity magnetic field can be taken as another future step to investigate the capability of this non-invasive diagnostic tool.

In conclusion, our results indicate that comparing the total of choline and creatinine to citrate ratio, can acceptably contribute to differentiation of prostatitis and PCa. According to the findings, it can be concluded that MRS can be used as a suitable and noninvasive tool with high level of sensitivity, specificity and accuracy for differentiating PCa and prostatitis.

Previous studies have noted the sensitivity, specificity, and accuracy of spectroscopy in the diagnosis of PCa or changes in levels of metabolites. However, none of them has investigated the accuracy of MRS in distinguishing cancer from benign prostate lesions. So for the first time, this study investigated the accuracy of MRS techniques in differentiation of cancer from prostatitis.

Authors' Contribution
Design of the work: MZ. Data collection: ZF, JFA, SD, SMH and MS. Data analysis and interpretation: MZ, ZF, JFA, BC, SMH and MMG. Drafting the article: MZ, ZF, and JFA. Critical revision of the article: MZ, ZF, JFA and BC.

Conflict of Interest Disclosures
None.

References
1. Futterer JJ, Heijmink SW, Scheenen TW, Veltman J, Huisman HJ, Vos P, et al. Prostate cancer localization with dynamic contrast-enhanced MR imaging and proton MR spectroscopic imaging. Radiology. 2006;241(2):449-58. doi: 10.1148/radiol.2412051866.
2. Panebianco V, Barchetti F, Musio D, Forte V, Pace A, De Felice F, et al. Metabolic atrophy and 3-T 1 H-magnetic resonance spectroscopy correlation after radiation therapy for prostate cancer. BJU international. 2014;114(6):852-9. doi: 10.1111/bju.12553
3. Testa C, Schiavina R, Lodi R, Salizzoni E, Corti B, Farsad M, et al. Prostate cancer: sextant localization with MR imaging, MR spectroscopy, and 11C-choline PET/CT. Radiology. 2007;244(3):797-806. doi: 10.1148/radiol.2443061063.
4. Bauman G, Belhocine T, Kovacs M, Ward A, Beheshti M, Rachinsky I. 18 F-fluorocholine for prostate cancer imaging: a systematic review of the literature. Prostate cancer and prostatic diseases. 2012;15(1):45. doi: 10.1038/pcan.2011.35.
5. Riches S, Payne G, Morgan V, Dearnaley D, Morgan S, Partridge M, et al. Multivariate modelling of prostate cancer combining magnetic resonance derived T2, diffusion, dynamic contrast-enhanced and spectroscopic parameters. Eur Radiol. 2015;25(5):1247-56. doi: 10.1007/s00330-014-3479-0.
6. Ahmed H, El-Shater Bosaily A, Brown L, Gabe R, Kaplan R, Parmar M, et al. PROMIS study group: Diagnostic accuracy of multi-parametric MRI and TRUS biopsy in prostate cancer (PROMIS): A paired validating confirmatory study. Lancet. 2017;389(10071):815-822. doi: 10.1016/S0140-6736(16)32401-1.
7. Jacobs MA, Ouwerkerk R, Petrowski K, Macura KJ. Diffusion weighted imaging with ADC mapping and spectroscopy in prostate cancer. Top Magn Reson Imaging. 2008;19(6):261-72. doi: 10.1097/RMR.0b013e3181aa6b50.
8. Heidenreich A, Bellmunt J, Bolla M, Joniau S, Mason M, Matveev V, et al. EAU guidelines on prostate cancer. Part 1: screening, diagnosis, and treatment of clinically localised disease. Eur Urol. 2011;59(1):61-71. doi: 10.1016/j.eururo.2010.10.039.
9. Lee DH, Koo KC, Lee SH, Rha KH, Choi YD, Hong SJ, et al. Tumor lesion diameter on diffusion weighted magnetic resonance imaging could help predict insignificant prostate cancer in patients eligible for active surveillance: preliminary analysis. J Urol. 2013;190(4):1213-7. doi: 10.1016/j.juro.2013.03.127.
10. Shukla-Dave A, Hricak H, Kattan MW, Pucar D, Kuroiwa K, Chen HN, et al. The utility of magnetic resonance imaging and spectroscopy for predicting insignificant prostate cancer: an initial analysis. BJU Int. 2007;99(4):786-93. doi: 10.1111/j.1464-410X.2007.06689.x.
11. Kumar V, Jagannathan NR, Thulkar S, Kumar R. Prebiopsy magnetic resonance spectroscopy and imaging in the diagnosis of prostate cancer. Int J Urol. 2012;19(7):602-13. doi: 10.1111/j.1442-2042.2012.02995.x.
12. Jung JA, Coakley FV, Vigneron DB, Swanson MG, Qayyum A, Weinberg V, et al. Prostate depiction at endorectal MR spectroscopic imaging: investigation of a standardized evaluation system. Radiology. 2004;233(3):701-8. doi:

10.1148/radiol.2333030672.

13. Sciarra A, Panebianco V, Ciccariello M, Salciccia S, Lisi D, Osimani M, et al. Magnetic resonance spectroscopic imaging (1H-MRSI) and dynamic contrast-enhanced magnetic resonance (DCE-MRI): pattern changes from inflammation to prostate cancer. Cancer Invest. 2010;28(4):424-32. doi: 10.3109/07357900903287048.

14. Fütterer JJ, Scheenen TW, Heijmink SW, Huisman HJ, Hulsbergen-Van de Kaa CA, Witjes JA, et al. Standardized threshold approach using three-dimensional proton magnetic resonance spectroscopic imaging in prostate cancer localization of the entire prostate. Invest Radiol. 2007;42(2):116-22. doi: 10.1097/01.rli.0000251541.03822.bb.

15. Lee SA, Bae SH, Ryoo HM, Jung HY, Jang SB, Kum YS. Primary retroperitoneal mucinous cystadenocarcinoma: a case report and review of the literature. Korean J Intern Med. 2007;22(4):287-91. doi: 10.3904/kjim.2007.22.4.287.

16. Chen M, Dang H-D, Wang J-Y, Zhou C, Li S-Y, Wang W-C, et al. Prostate cancer detection: comparison of T2-weighted imaging, diffusion-weighted imaging, proton magnetic resonance spectroscopic imaging, and the three techniques combined. Acta Radiol. 2008;49(5):602-10. doi: 10.1080/02841850802004983.

17. Jagannathan D, Indiran V. Accuracy of Diffusion Weighted Images and MR Spectroscopy in Prostate Lesions–Our Experience with Endorectal Coil on 1.5 T MRI. J Clin Diagn Res. 2017;11(5):TC10. doi: 10.7860/JCDR/2017/27754.9825.

18. Kim JK, Kim DY, Lee YH, Sung NK, Chung DS, Kim OD, et al. In vivo differential diagnosis of prostate cancer and benign prostatic hyperplasia: localized proton magnetic resonance spectroscopy using external-body surface coil. Magn Reson Imaging. 1998;16(10):1281-8. doi: 10.1016/s0730-725x(98)00110-6.

19. Garcia-Segura J, Sanchez-Chapado M, Ibarburen C, Viano J, Angulo J, Gonzalez J, et al. In vivo proton magnetic resonance spectroscopy of diseased prostate: spectroscopic features of malignant versus benign pathology. Magn Reson Imaging. 1999;17(5):755-65. doi: 10.1016/s0730-725x(99)00006-5.

20. Barentsz JO, Richenberg J, Clements R, Choyke P, Verma S, Villeirs G, et al. ESUR prostate MR guidelines 2012. Eur Radiol. 2012;22(4):746-57. doi: 10.1007/s00330-011-2377-y.

21. van der Graaf M, Schipper RG, Oosterhof GO, Schalken JA, Verhofstad AA, Heerschap A. Proton MR spectroscopy of prostatic tissue focused on the etection of spermine, a possible biomarker of malignant behavior in prostate cancer. MAGMA. 2000;10(3):153-9. doi: 10.1007/bf02590640.

22. Bellomo G, Marcocci F, Bianchini D, Mezzenga E, D'Errico V, Menghi E, et al. MR spectroscopy in prostate cancer: new algorithms to optimize metabolite quantification. PLoS One. 2016;11(11):e0165730. doi: 10.1371/journal.pone.0165730.

23. Verma S, Rajesh A, Fütterer JJ, Turkbey B, Scheenen TW, Pang Y, et al. Prostate MRI and 3D MR spectroscopy: how we do it. AJR Am J Roentgenol. 2010;194(6):1414-26. doi: 10.2214/AJR.10.4312.

24. Zhang T, Hu C, Chen J, Xu Z, Shen J. Differentiation Diagnosis of Hypo-Intense T2 Area in Unilateral Peripheral Zone of Prostate Using Magnetic Resonance Spectroscopy (MRS): Prostate Carcinoma versus Prostatitis. Med Sci Monit. 2017;23:3837-3843. doi: 10.12659/MSM.903123.

25. Claus FG, Hricak H, Hattery RR. Pretreatment evaluation of prostate cancer: role of MR imaging and 1H MR spectroscopy. Radiographics. 2004;24 Suppl 1:S167-80. doi: 10.1148/24si045516.

26. Panigrahy A, Nelson Jr MD, Finlay JL, Sposto R, Krieger MD, Gilles FH, et al. Metabolism of diffuse intrinsic brainstem gliomas in children. Neuro Oncol. 2008;10(1):32-44. doi: 10.1215/15228517-2007-042.

27. Heerschap A, Jager GJ, Graaf M, Barentsz JO, Rosette Jdl, Oosterhof G, et al. In vivo proton MR spectroscopy reveals altered metabolite content in malignant prostate tissue. Anticancer Res. 1997;17(3A):1455-60.

28. Zhang TH, Hu CH, Chen JX, Xu ZD, Shen JK. Differentiation Diagnosis of Hypo-Intense T2 Area in Unilateral Peripheral Zone of Prostate Using Magnetic Resonance Spectroscopy (MRS): Prostate Carcinoma versus Prostatitis. Med Sci Monit. 2017;23:3837-3843. doi: 10.12659/MSM.903123.

29. Kurhanewicz J, Vigneron DB. Advances in MR spectroscopy of the prostate. Magn Reson Imaging Clin N Am. 2008;16(4):697-710. doi: 10.1016/j.mric.2008.07.005.

30. Meier-Schroers M, Kukuk G, Wolter K, Decker G, Fischer S, Marx C, et al. Differentiation of prostatitis and prostate cancer using the Prostate Imaging—Reporting and Data System (PI-RADS). Eur J Radiol. 2016;85(7):1304-11. doi: 10.1016/j.ejrad.2016.04.014.

31. Hricak H, Choyke PL, Eberhardt SC, Leibel SA, Scardino PT. Imaging prostate cancer: a multidisciplinary perspective. Radiology. 2007;243(1):28-53. doi: 10.1148/radiol.2431030580.

32. Dittrich R, Kurth J, Decelle E, DeFeo E, Taupitz M, Wu S, et al. Assessing prostate cancer growth with citrate measured by intact tissue proton magnetic resonance spectroscopy. Prostate Cancer Prostatic Dis. 2012;15(3):278-82. doi: 10.1038/pcan.2011.70.

33. Kurhanewicz J, Swanson MG, Nelson SJ, Vigneron DB. Combined magnetic resonance imaging and spectroscopic imaging approach to molecular imaging of prostate cancer. J Magn Reson Imaging. 2002;16(4):451-63. doi: 10.1002/jmri.10172.

34. Kurhanewicz J, Vigneron DB, Males RG, Swanson MG, Kyle KY, Hricak H. The prostate: MR imaging and spectroscopy: present and future. Radiol Clin North Am. 2000;38(1):115-38.

35. Cirillo S, Petracchini M, Della Monica P, Gallo T, Tartaglia V, Vestita E, et al. Value of endorectal MRI and MRS in patients with elevated prostate-specific antigen levels and previous negative biopsies to localize peripheral zone tumours. Clin Radiol. 2008;63(8):871-9. doi: 10.1016/j.crad.2007.10.020.

36. Wang W, Hu Y, Lu P, Li Y, Chen Y, Tian M, et al. Evaluation of the diagnostic performance of magnetic resonance spectroscopy in brain tumors: a systematic review and meta-analysis. PLoS One. 2014;9(11):e112577. doi: 10.1371/journal.pone.0112577.

37. Amsellem-Ouazana D, Younes P, Conquy S, Peyromaure M, Flam T, Debré B, et al. Negative prostatic biopsies in patients with a high risk of prostate cancer: is the combination of endorectal MRI and magnetic resonance spectroscopy imaging (MRSI) a useful tool? A preliminary study. PLoS One. 2014;9(11):e112577. doi: 10.1371/journal.pone.0112577.

38. Ghafoori M, Rasteh M. The relationship between choline plus creatine- to-citrate ratio in magnetic resonance spectroscopy with the invasion of prostate cancer TUMJ. 2012;70(9):571-6.

39. Kobus T, Hambrock T, Hulsbergen-Van de Kaa CA, Wright AJ, Barentsz JO, Heerschap A, et al. In vivo assessment of prostate cancer aggressiveness using magnetic resonance spectroscopic imaging at 3 T with an endorectal coil. Eur Urol. 2011;60(5):1074-80. doi: 10.1016/j.eururo.2011.03.002.

40. Cheng LL, Burns MA, Taylor JL, He W, Halpern EF, McDougal WS, et al. Metabolic characterization of human prostate cancer with tissue magnetic resonance spectroscopy. Cancer Res. 2005;65(8):3030-4. doi: 1 0.1158/0008-5472.CAN-04-4106.

41. Yu KK, Scheidler J, Hricak H, Vigneron DB, Zaloudek CJ, Males RG, et al. Prostate cancer: prediction of extracapsular extension with endorectal MR imaging and three-dimensional proton MR spectroscopic imaging. Radiology. 1999;213(2):481-8. doi: 10.1148/radiology.213.2.r99nv26481.

42. Verma A, Kumar I, Verma N, Aggarwal P, Ojha R. Magnetic resonance spectroscopy—revisiting the biochemical and molecular milieu of brain tumors. BBA Clin. 2016;5:170-8. doi: 10.1016/j.bbacli.2016.04.002.

43. Mueller-Lisse UG, Vigneron DB, Hricak H, Swanson MG, Carroll PR, Bessette A, et al. Localized prostate cancer: effect of hormone deprivation therapy measured by using combined three-dimensional 1H MR spectroscopy and MR imaging: clinicopathologic case-controlled study. Radiology. 2001;221(2):380-90. doi: 1 0.1148/radiol.2211001582

44. Yuen J, Thng C, Tan P, Khin L, Phee S, Xiao D, et al. Endorectal magnetic resonance imaging and spectroscopy for the detection of tumor foci in men with prior negative transrectal ultrasound prostate biopsy. J Urol. 2004;171(4):1482-6.10.1097/01.ju.0000118380.90871.ef.

45. Sciarra A, Panebianco V, Salciccia S, Osimani M, Lisi D, Ciccariello M, et al. Role of dynamic contrast-enhanced magnetic resonance (MR) imaging and proton MR spectroscopic imaging in the detection of local recurrence after radical prostatectomy for prostate cancer. Eur Urol. 2008;54(3):589-600. doi: 10.1016/j.eururo.2007.12.034.

46. Haffner J, Lemaitre L, Puech P, Haber GP, Leroy X, Jones JS, et al. Role of magnetic resonance imaging before initial biopsy: comparison of magnetic resonance imaging-targeted and systematic biopsy for significant prostate cancer detection. BJU Int. 2011;108(8 Pt 2):E171-8. doi: 10.1111/j.1464-410X.2011.10112.x.

47. Aydin H, Kizilgöz V, Tatar IG, Damar Ç, Ugan AR, Paker I, et al. Detection of prostate cancer with magnetic resonance imaging: optimization of T1-weighted, T2-weighted, dynamic-enhanced T1-weighted, diffusion-weighted imaging apparent diffusion coefficient mapping sequences and MR spectroscopy, correlated with biopsy and histopathological findings. J Comput Assist Tomogr. 2012;36(1):30-45. doi: 10.1097/RCT.0b013e31823f6263.

48. Caivano R, Cirillo P, Balestra A, Lotumolo A, Fortunato G, Macarini L, et al. Prostate cancer in magnetic resonance imaging: diagnostic utilities of spectroscopic sequences. Journal of medical imaging and radiation oncology. J Med Imaging Radiat Oncol. 2012;56(6):606-16. doi: 10.1111/j.1754-9485.2012.02449.x.

49. Roy C, Foudi F, Charton J, Jung M, Lang H, Saussine C, et al. Comparative sensitivities of functional MRI sequences in detection of local recurrence of prostate carcinoma after radical prostatectomy or external-beam radiotherapy. AJR Am J Roentgenol. 2013;200(4):W361-8. doi: 10.2214/AJR.12.9106.

50. Cha D, Kim CK, Park SY, Park JJ, Park BK. Evaluation of suspected soft tissue lesion in the prostate bed after radical prostatectomy using 3 T multiparametric magnetic resonance imaging. Magnetic resonance imaging. 2015;33(4):407-12. doi: 10.1016/j.mri.2014.12.003.

51. Kitajima K, Hartman RP, Froemming AT, Hagen CE, Takahashi N, Kawashima A. Detection of local recurrence of prostate cancer after radical prostatectomy using endorectal coil MRI at 3 T: addition of DWI and dynamic contrast enhancement to T2-weighted MRI. AJR Am J Roentgenol. 2015;205(4):807-16. doi: 10.2214/AJR.14.14275.

52. Vigneault E, Mbodji K, Racine LG, Chevrette E, Lavallee MC, Martin AG, et al. Image-Guided High-Dose-Rate (HDR) Boost Localization Using MRI/MR Spectroscopy: A Correlation Study with Biopsy. Cureus. 2016;8(9):e795. doi: 10.7759/cureus.795.

53. Sandgren K, Westerlinck P, Jonsson JH, Blomqvist L, Karlsson CT, Nyholm T, et al. Imaging for the detection of locoregional recurrences in biochemical progression after radical prostatectomy—a systematic review. Eur Urol Focus. 2019;5(4):550-560. doi: 10.1016/j.euf.2017.11.001.